Performance of an Axial-flux Permanent-magnet Synchronous Generator with Double-sided Rotor and Coreless Armature

T. F. Chan[1], Weimin Wang[1] and L. L. Lai[2]
[1]Department of EE, the Hong Kong Polytechnic University, Hung Hom, Hong Kong, China
[2]Energy Systems Group, School of Mathematics and Engineering Sciences, City University London, UK
eetfchan@polyu.edu.hk, eewmwang@polyu.edu.hk, l.l.lai@city.ac.uk

Abstract — This paper presents the performance of axial flux permanent-magnet synchronous generator (AFPMSG) with double rotor. The AFPMSG has 16 poles on each rotor and a compact disk armature winding with 12 coils and without iron core. The field distribution and load performance are computed for a prototype machine based on a two-dimensional, time-stepping finite element method. The armature reaction effect is computed for the first time for an AFPMSG with a fractional slot, coreless armature winding. The computed waveforms and load characteristic have been verified by experiments on a prototype generator.

I. Introduction

Axial flux permanent magnet synchronous generators (AFPMSG), in which air gaps lie in the axial direction of the rotor rather than its periphery, lend themselves to be mechanically suitable for both high-speed operation [1] and low-speed operation [2] with a high efficiency. In this paper, a prototype AFPMSG with double-sided permanent magnet rotor and coreless armature winding with fractional slot, non-overlapping coils is studied. As shown in Fig. 1, the coreless stator is sandwiched between two rotors with surface-mounted, neodymium-iron-boron (NdFeB) magnets. Each rotor has 16 magnetic poles, while the armature winding has 12 concentrated, non-overlapping coils which are embedded in epoxy resin for mechanical strength. It is apparent that the AFPMSG has a fractional slot winding with characteristic ratio $1/y$ [3], where $y = 4$. That is, the winding repeats itself over a distance of four pole-pitches. Finite element method (FEM) is used for prediction of the magnetic field distribution and generator performance. For prediction of load performance, a time-stepping, coupled field-circuit approach is used. The study also sheds light on the armature reaction effect of the coreless prototype generator with concentrated, non-overlapping coils. The computed results are verified by experiments where possible.

II. Analysis

The above observation suggests that for periodic conditions to be applied successfully, the time-stepping FE model has to include at least four poles. In order to reduce the scale of the problem, two-dimensional finite element analysis (2-D FEA) will be conducted for a cutting plane at the mean radius of the generator.

There are six armature conductor regions in the FE model of the AFPMSG shown in Fig. 2. The nodes of each region comprises three degrees of freedom (DOFs), namely, the vector potential A_z, the current (CURR) and the electromotive force (EMF). The EMF and CURR DOF of all the nodes in a given region should each be unified as a single variable in the coupled field-circuit FE computations.

There are 8466 elements and 22991 nodes in the 2D analysis. Since there is no flux linkage outside the modeled region, the Neumann boundary condition can be assigned to the upper and lower exterior nodes. Periodic boundary condition is applied to nodes on the leftmost rightmost exterior nodes. The number of nodes located on Neumann boundary is 514, the number of nodes located on period boundary condition is 210, and the number of conductor regions is 6. The total variables is thus 22991-514-210/2+2×6=22384. With a chosen time-step is 0.0167 ms, the computing time is about 31.5 h for a typical load.

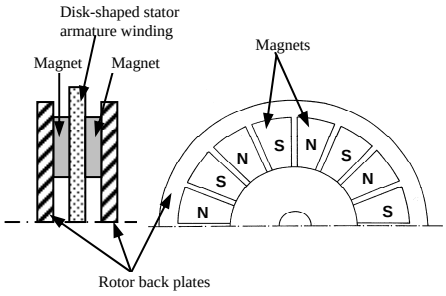

Fig. 1. Half cross-section of prototype AFPMSG

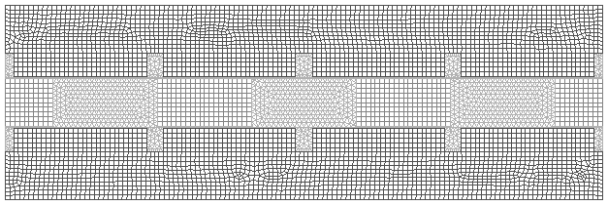

Fig. 2. Geometric model and meshing of AFPMSG for FEA

III. Results

A. Flux plots

Fig. 3 shows the flux plot of the AFPMSG with double-sided rotor under no-load condition. It is observed that the flux density distribution is symmetrical about the center plane of the stator armature, across which the flux lines pass normally. Null points of flux density also occur on this plane at the interpolar circumferential positions. The flux densities in the rotor back plates are high at interpolar positions.

A close examination of the field plot in Fig. 4 shows that some asymmetry in the field distribution exists due to the effect of armature reaction. There is a noticeable shift in the

positions of zero flux density points along the mean position of the disk winding.

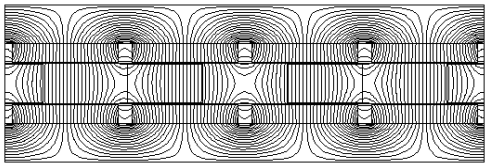

Fig. 3. Flux plot of AFPMSG at no load

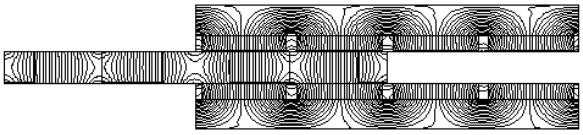

Fig.4. Flux plot of AFPMSG at rated load

B. Flux density

Fig. 5 shows the variation of axial component of flux density B_z in the circumferential direction along the mean radius. In the mean air gap (z = 5.25 mm), the waveform is flat-topped, while at the mean position of the disk winding (z = 0), the waveform becomes more sinusoidal. Since most of the conductors are within the region –3 mm < z < 3 mm, it is expected that the generated e.m.f. from the AFPMSG with double-sided rotor should be quite sinusoidal. The waveform of B_z at z = 8 mm (magnet region) and z = 11.5 mm (rotor back plate) are double-peaked and saddle-shaped, due to the concentration of flux lines at both edges of the magnets.

Fig. 6 shows the armature reaction flux density in the AFPMSG at the time instant when the instantaneous current in phase A is maximum. The armature reaction flux density is relatively small because of the air-cored winding configuration. Due to the use of fractional slot winding, the flux density distribution is not symmetrical over a physical pole pitch, giving rise to a series of armature reaction harmonics.

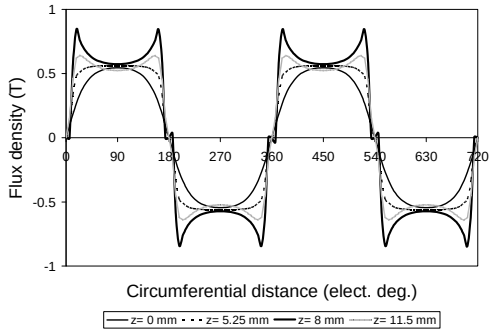

Fig. 5. Circumferential variations of B_z at different axial positions

C. Computed voltage waveforms

Fig. 7 shows the computed waveforms of the phase voltage and line voltage when the AFPMSG is on no load. The flat-topped phase voltage waveform is due to the relatively large third harmonic in the air gap flux density. The experimental waveforms in Fig. 8 confirm the accuracy of the FEA.

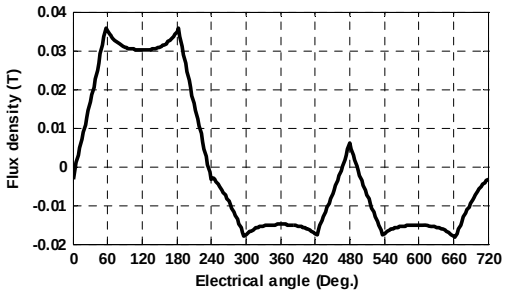

Fig. 6. Axial component of armature reaction flux density: I_a = -8.34 A, I_b = I_c = 4.17 A

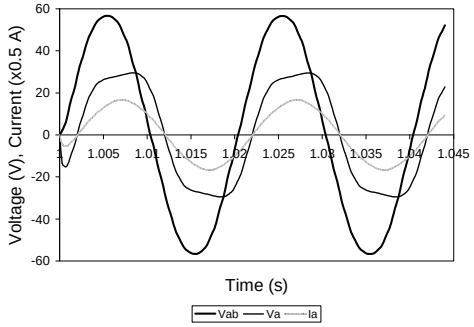

Fig. 7. Computed line voltage, phase voltage and line current waveforms at rated speed and rated load current

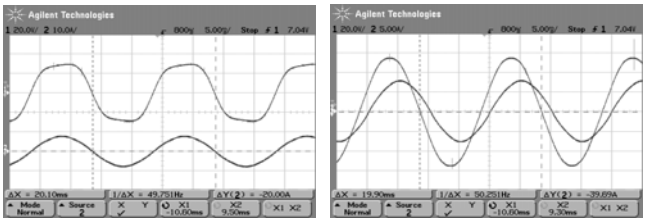

(a) (b)

Fig. 8. Experimental waveforms: (a) Phase voltage and line current (b) Line voltage and current

IV. CONCLUSIONS

The performance of an AFPMSG with double-sided rotor and coreless armature has been studied using time-stepping 2-D FEA. Further details of field analysis and experimental results, such as torque, voltage regulation, and efficiency, will be reported in the extended paper.

V. ACKNOWLEDGMENT

The work was fully supported by a grant from the Research Committee, The Hong Kong Polytechnic University, Hong Kong, China (Project No. G-YG31).

VI. REFERENCES

[1] Rong-Jie Wang, M.J. Kamper, K.Van der Westhuizen and J.F. Gieras, "Optimal design of a coreless stator axial flux permanent-magnet generator" *IEEE Trans. Magn.*, 41(1): 55-64, 2005.

[2] J. R. Bumby, R. Martin, M. A. Mueller, E. Spooner, N. L. Brown and B. J. Chalmers, "Electromagnetic design of axial-flux permanent magnet machines," *IEE Proc. – Elect. Power Appl.*, 151(2): 151–159, 2004.

[3] W. S. Wood, *Theory of Electrical Machines.* London: Butterworths Scientific Publications, 1958.